



ORIGINAL ARTICLE

A note on thermal-diffusion and chemical reaction effects on MHD pulsating flow in a porous channel with slip and convective boundary conditions

S. Srinivas ^a, T. Malathy ^b, A. Subramanyam Reddy ^{a,*}

^a Fluid Dynamics Division, School of Advanced Sciences, VIT University, Vellore 632014, India

^b Muthurangam Government Arts & Science College, Vellore 632002, India

Received 28 January 2014; accepted 30 March 2014

KEYWORDS

Porous channel;
Chemical reaction;
Convective boundary;
Soret number;
Slip parameter

Abstract The present note investigates the effects of chemical reaction and Soret effects on hydromagnetic laminar viscous pulsating flow in a porous channel with slip and convective boundary conditions. The governing equations are solved analytically and the expressions for velocity, temperature, concentration, Nusselt number and Sherwood number distributions are obtained. The effects of various pertinent parameters on flow variables have been discussed numerically and explained graphically. Analysis indicates that the temperature distribution decreases for a given increase in heat transfer Biot number and Prandtl number while it increases with an increase in Hartmann number. Further, the concentration distribution increases with an increase in the mass transfer Biot number, Soret number and the heat transfer Biot number, while it decreases for a given increase in the chemical reaction parameter.

© 2014 Production and hosting by Elsevier B.V. on behalf of King Saud University.

1. Introduction

Studies pertaining to fluid flow in a porous pipe or channel have received much attention of several researchers in recent years due to their applications in technological as well as biological flows, with a view to understand some practical phenomena such as transpiration cooling, gaseous diffusion,

circulatory system and respiratory system (Berman, 1953; Terrill, 1964; Cox, 1991). Particularly, the pulsatile flow in a porous channel is important to understand the process of dialysis of blood in an artificial kidney Radhakrishnamacharya and Maiti (1977). Radhakrishnamacharya and Maiti (1977) have made an investigation of heat transfer to pulsatile flow in a porous channel. In this investigation, the walls were maintained at uniform temperatures and fluid was injected through one wall and removed at the opposite wall at the same rate. Malathy and Srinivas (2008) studied the characteristics of pulsatile hydromagnetic flow of an Oldroyd fluid with heat transfer. It is well known that the slip effect at porous boundaries cannot be neglected, especially in the case of high permeable porous media (Beavers and Joseph, 1967; Chen and Zhu, 2008; Hayat et al., 2012; Akbar et al., 2012a). Chellam et al. (1992) investigated the effect of fluid flow and mass transfer

* Corresponding author. Tel.: +91 416 2202514.

E-mail address: anala.subramanyamreddy@gmail.com (A. Subramanyam Reddy).

Peer review under responsibility of King Saud University.



Production and hosting by Elsevier

on slip at uniformly porous boundary. [Xinhui et al. \(2012\)](#) have studied the effects of slip velocity on a micropolar fluid through a porous channel with expanding or contracting walls by using the homotopy analysis method. [Hayat et al. \(2010\)](#) analyzed the Simultaneous effects of slip and heat transfer on the peristaltic flow. [Akbar et al. \(2012b\)](#) examined the effects of thermal and velocity slip on the peristaltic flow of a Johnson–Segalman fluid in an inclined asymmetric channel.

In many transport process in nature, flow is driven by density differences caused by temperature gradient, chemical composition (concentration) gradient and material composition. The temperature gradients can cause the mass fluxes, it is called the Soret effect (thermal-diffusion effect). The Soret effect has been found to be of importance as it is utilized for isotope separation and, in a mixture of gases of light molecular (H_2, He) and medium molecular weight (N_2, air) ([Narayana et al., 2008](#); [Hayat et al., 2011](#); [Dursunkaya and Worek, 1992](#)). [Chamka and Nakhi \(2008\)](#) have studied the convection and radiation interaction along a permeable surface immersed in a porous medium in the presence of Soret and Dufour’s effects. [Srinivas et al. \(2012\)](#) and several references therein have analyzed the effects of thermal-diffusion and diffusion-thermo effects on two-dimensional viscous flow in a porous channel with slowly expanding or contracting walls with weak permeability. [Akbar and Nadeem \(2012\)](#) studied the characteristics of heating scheme and mass transfer on the peristaltic flow for an Eyring-Powell fluid in an endoscope. Recently, [Mustafa et al. \(2014\)](#) have made Numerical investigation on mixed convective peristaltic flow of fourth grade fluid with Dufour and Soret effects. The convective boundary condition is more general and pragmatic, especially with respect to several engineering and industrial processes like transpiration cooling process and material drying ([Yao et al., 2011](#); [Chinyoka and Makinde, 2011](#)). [Makinde \(2009\)](#) and several references therein) obtained numerical solutions for the unsteady hydromagnetic generalized couette flow of a reactive third-grade fluid with asymmetric convective cooling. [Akbar \(2013\)](#) studied MHD Eyring Prandtl fluid with convective boundary conditions in small intestines. [Nadeem et al. \(2014\)](#) obtained optimized analytical solution for oblique flow of a Casson-nanofluid with convective boundary conditions.

It is noted through the survey of literature that no attempt has been made for studying the combined effects of Soret and chemical reaction effects on pulsating MHD slip flow of viscous fluid in a porous channel with convective boundary conditions. Such consideration is of great value in engineering and science research. The main motivation for this investigation stems from the previous studies ([Radhakrishnamacharya and Maiti, 1977](#); [Xinhui et al., 2012](#); [Hayat et al., 2010](#); [Chamka and Nakhi, 2008](#); [Mustafa et al., 2014](#); [Makinde, 2009](#); [Nadeem et al., 2014](#)). Keeping in view, the wide range of applications both in engineering and science, an attempt is made here to study the effects of Soret and chemical reaction on pulsating MHD slip flow in a porous channel with convective boundary.

2. Formulation of the problem

Consider the pulsatile flow of the electrically conducting fluid in a porous channel, which is driven by the unsteady pressure gradient

$$-\frac{1}{\rho} \frac{\partial p}{\partial x} = A(1 + \varepsilon \exp(i\omega t)) \tag{1}$$

where A is a known constant, $\varepsilon (\ll 1)$ is a suitable chosen positive quantity and ω is the frequency and ρ is density. As shown in [Fig. 1](#) the x -axis is taken along one wall and the y -axis is normal to it. The channel walls posses the characteristics of convective type boundary condition. The lower wall $y = 0$ maintains a temperature T_1 which represents the convective boundary condition $-\kappa \frac{\partial T}{\partial y} = h_f(T - T_1)$ and a concentration C_1 which represents the convective boundary $-D \frac{\partial C}{\partial y} = h_m(C - C_1)$. The upper wall $y = h$ maintains a temperature T_0 which represents the convective boundary condition $-\kappa \frac{\partial T}{\partial y} = h_f(T - T_0)$ and a concentration C_0 which represents the convective boundary $-D \frac{\partial C}{\partial y} = h_m(C - C_0)$. A magnetic field of uniform strength B_0 is applied perpendicular to the walls. On one plate some fluid is injected with a velocity v and sucked at the opposite plate at the same rate. Under these assumptions, the governing equations are [Radhakrishnamacharya and Maiti \(1977\)](#),

$$\frac{\partial u}{\partial t} + v \frac{\partial u}{\partial y} = -\frac{1}{\rho} \frac{\partial p}{\partial x} + \nu \frac{\partial^2 u}{\partial y^2} - \frac{\sigma B_0^2}{\rho} u \tag{2}$$

$$0 = -\frac{1}{\rho} \frac{\partial p}{\partial y} \tag{3}$$

$$\rho c_p \left(\frac{\partial T}{\partial t} + v \frac{\partial T}{\partial y} \right) = \kappa \frac{\partial^2 T}{\partial y^2} + \mu \left(\frac{\partial u}{\partial y} \right)^2 \tag{4}$$

$$\frac{\partial C}{\partial t} + v \frac{\partial C}{\partial y} = D \frac{\partial^2 C}{\partial y^2} + \frac{Dk_T}{T_m} \frac{\partial^2 T}{\partial y^2} - k_1 C \tag{5}$$

where u is the velocity, ν is the kinematic viscosity, σ is the electrical conductivity, B_0 is the strength of applied magnetic field, μ is the dynamic viscosity, c_p is the specific heat at constant pressure, κ is the thermal conductivity, T, C are the temperature and concentration of the fluid respectively, D is the coefficient of mass diffusivity, k_1 is the first order chemical reaction rate, k_T is the thermal diffusion ratio and T_m is the mean temperature of the fluid. The appropriate boundary conditions are ([Chen and Zhu, 2008](#); [Xinhui et al., 2012](#); [Chinyoka and Makinde, 2011](#); [Makinde, 2009](#)),

$$\begin{aligned} u = \frac{\sqrt{k}}{\alpha} \frac{\partial u}{\partial y}, \quad -\kappa \frac{\partial T}{\partial y} = h_f(T - T_1), \\ -D \frac{\partial C}{\partial y} = h_m(C - C_1) \quad \text{at } y = 0 \end{aligned} \tag{6}$$

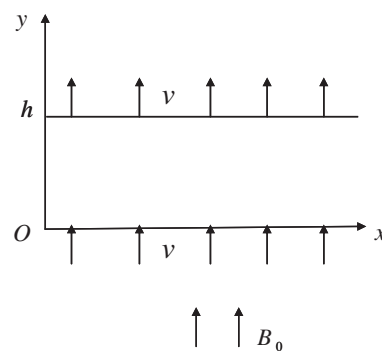


Figure 1 Schematic diagram of the model.

$$u = -\frac{\sqrt{k}}{\alpha} \frac{\partial u}{\partial y}, \quad -\kappa \frac{\partial T}{\partial y} = h_f(T - T_0),$$

$$-D \frac{\partial C}{\partial y} = h_m(C - C_0) \quad \text{at } y = h \quad (7)$$

where k is the permeability of the porous walls, α is slip coefficient at the surface of the porous walls, h_f and h_m are heat and mass transfer coefficients respectively. The solution of the Eq. (2) is in the form Radhakrishnamacharya and Maiti (1977):

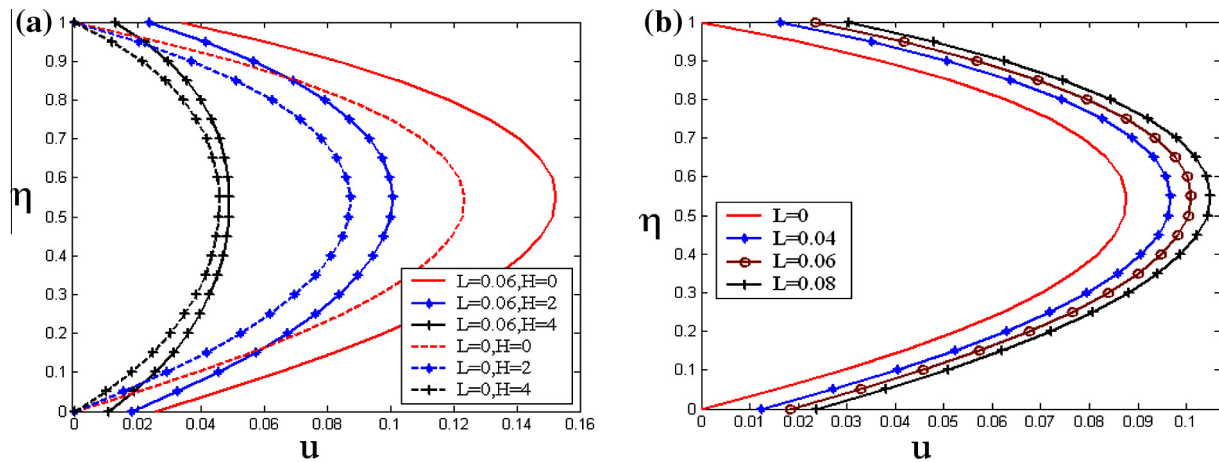


Figure 2 Velocity distribution for $\varepsilon = 0.01$, $\omega t = \pi/2$, $R = 1$, $M = 5$. (a) Effect of H and (b) Effect of L when $H = 2$.

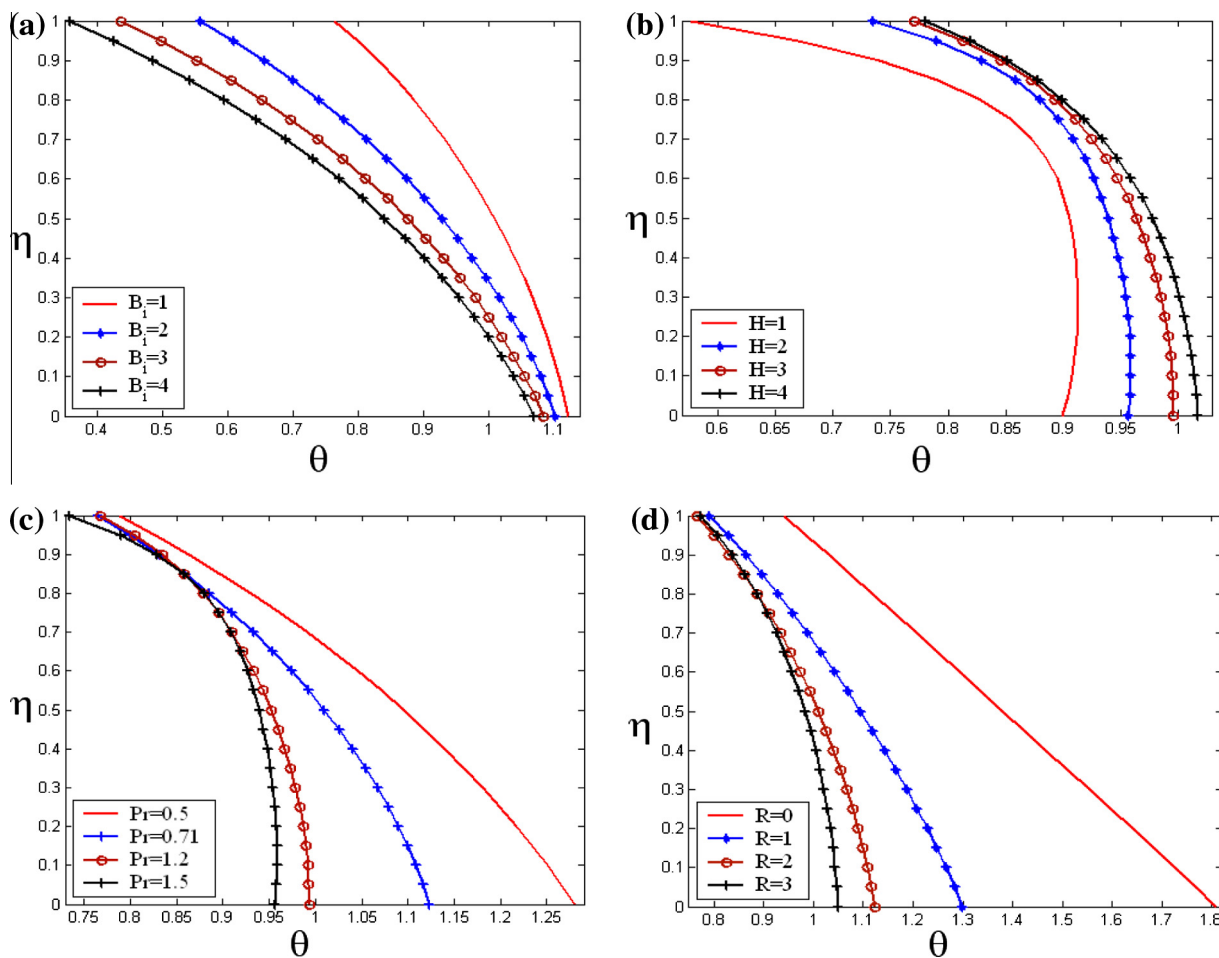


Figure 3 Temperature distribution for $M = 5$, $Ec = 5$, $L = 0.06$, $\varepsilon = 0.01$, $\omega t = \pi/2$. (a) Effect of B_i when $H = 2$, $Pr = 0.71$, $R = 2$, (b) Effect of H when $B_i = 1$, $Pr = 1.5$, $R = 2$, (c) Effect of Pr when $H = 2$, $B_i = 1$, $R = 2$ and (d) Effect of R when $H = 2$, $B_i = 1$, $Pr = 0.71$.

$$u = \frac{Ah^2}{\nu} (u_0 + \epsilon u_1 \exp(i\omega t)) \quad (8)$$

By introducing the non-dimensional temperature and concentration

$$\theta = \frac{T - T_0}{T_1 - T_0}, \quad \phi = \frac{C - C_0}{C_1 - C_0}, \quad (9)$$

the Eqs. (4) and (5) become

$$\frac{h^2}{\nu} \frac{\partial \theta}{\partial t} + R \frac{\partial \theta}{\partial \eta} = \frac{1}{Pr} \frac{\partial^2 \theta}{\partial \eta^2} + Ec \left(\frac{\partial(u_0 + \epsilon u_1 \exp(i\omega t))}{\partial \eta} \right)^2 \quad (10)$$

$$\frac{h^2}{\nu} \frac{\partial \phi}{\partial t} + R \frac{\partial \phi}{\partial \eta} = \frac{1}{Sc} \frac{\partial^2 \phi}{\partial \eta^2} + Sr \frac{\partial^2 \theta}{\partial \eta^2} - \gamma \phi - K_1. \quad (11)$$

where $\eta = \frac{y}{h}$, $R = \frac{v h}{\nu}$ is cross flow Reynolds number,

$Pr = \frac{\mu c_p}{k}$ is the Prandtl number, $Ec = \frac{(Ah^2/\nu)^2}{c_p(T_1 - T_0)}$ is the Eckert number, $Sc = \frac{\nu}{D}$ is the Schmidt number,

$Sr = \frac{Dk_T(T_1 - T_0)}{T_m \nu (C_1 - C_0)}$ is the Soret number, $\gamma = \frac{k_1 h^2}{\nu}$ is the chemical reaction parameter and

$K_1 = \frac{C_0 h^2}{\nu(C_1 - C_0)}$. The corresponding boundary conditions are

$$u = L \frac{\partial u}{\partial \eta}, \quad \frac{\partial \theta}{\partial \eta} = -B_i(\theta - 1), \quad \frac{\partial \phi}{\partial \eta} = -N(\phi - 1) \quad \text{at } \eta = 0 \quad (12)$$

$$u = -L \frac{\partial u}{\partial \eta}, \quad \frac{\partial \theta}{\partial \eta} = -B_i, \quad \frac{\partial \phi}{\partial \eta} = -N\phi \quad \text{at } \eta = 1 \quad (13)$$

where $L = \frac{\sqrt{k}}{2h}$ is the slip parameter, $B_i = \frac{h_i h}{k}$ is the heat transfer Biot number and $N = \frac{h_m h}{D}$ is the mass transfer Biot number.

3. Solution of the problem

In view of (8), the temperature θ and concentration ϕ can be assumed to have the form

$$\theta = \theta_0(\eta) + \epsilon \theta_1(\eta) \exp(i\omega t) + \epsilon^2 \theta_2(\eta) \exp(2i\omega t) \quad (14)$$

$$\phi = \phi_0(\eta) + \epsilon \phi_1(\eta) \exp(i\omega t) + \epsilon^2 \phi_2(\eta) \exp(2i\omega t). \quad (15)$$

On substituting Eqs. (8), (14) and (15) into Eqs. (2), (10) and (11), equating the coefficients of various powers of ϵ , we obtain

$$u_0'' - Ru_0' - H^2 u_0 + 1 = 0 \quad (16)$$

$$u_1'' - Ru_1' - (iM^2 + H^2) u_1 + 1 = 0 \quad (17)$$

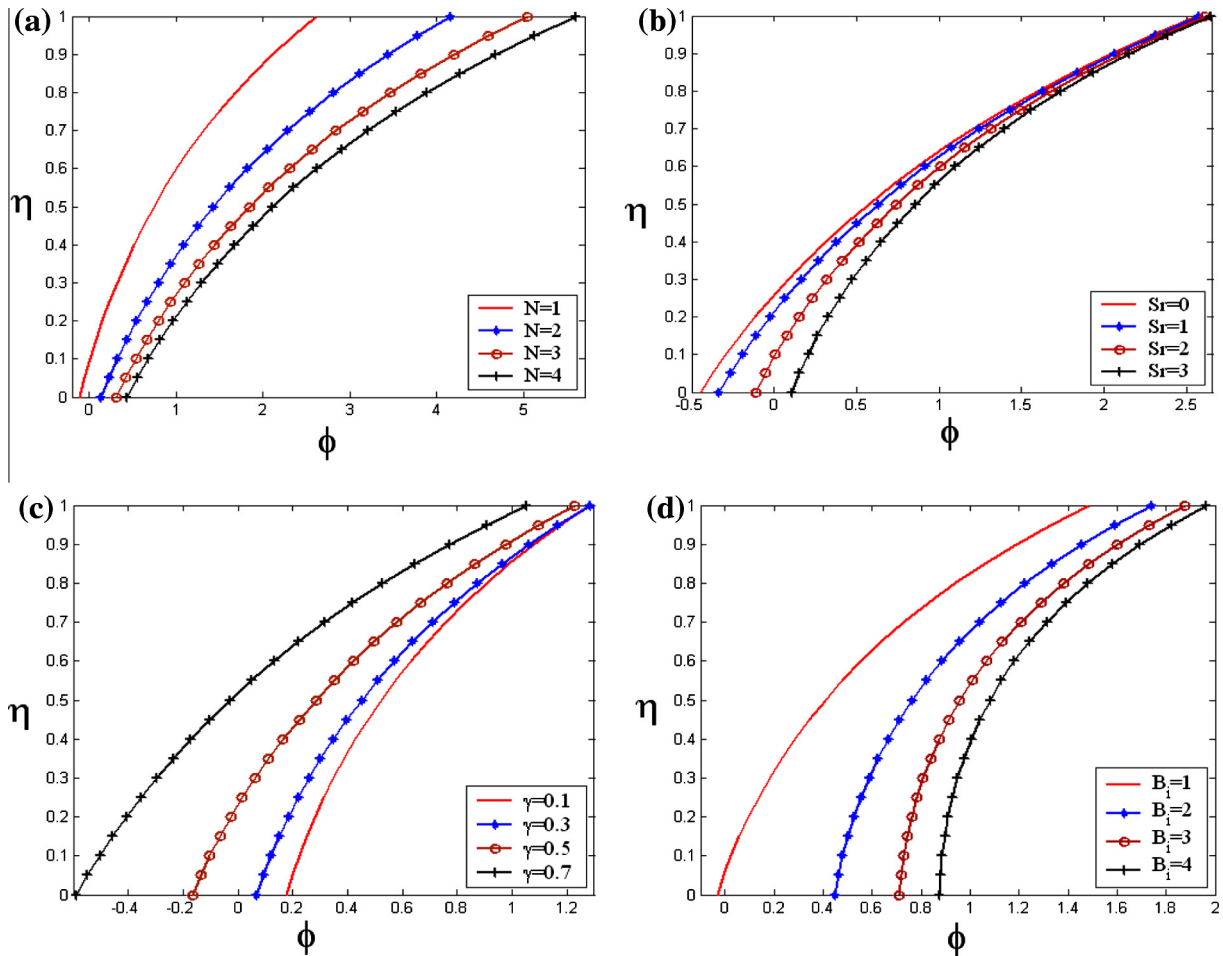


Figure 4 Concentration distribution for $L = 0.06$, $H = 2$, $Ec = 5$, $Pr = 0.71$, $R = 2$, $\epsilon = 0.01$, $K_1 = 0.001$, $\omega t = \pi/2$. (a) Effect of N when $B_i = 1$, $Sc = 0.62$, $\gamma = 0.3$, $Sr = 2$, (b) Effect of Sr when $B_i = 1$, $Sc = 0.62$, $\gamma = 0.3$, $N = 1$, (c) Effect of γ when $B_i = 1$, $Sc = 0.62$, $Sr = 2$, $N = 1$ and (d) Effect of B_i when $N = 1$, $Sc = 0.62$, $\gamma = 0.3$, $Sr = 2$.

$$\theta_0'' - RPr\theta_0' + EcPr u_0'^2 = 0 \tag{18}$$

$$\theta_1'' - RPr\theta_1' - iM^2Pr\theta_1 + 2EcPr u_0' u_1' = 0 \tag{19}$$

$$\theta_2'' - RPr\theta_2' - 2iM^2Pr\theta_2 + EcPr u_1'^2 = 0 \tag{20}$$

$$\phi_0'' - RSc\phi_0' - \gamma Sc\phi_0 - K_1 + ScSr\theta_0'' = 0 \tag{21}$$

$$\phi_1'' - RSc\phi_1' - (iM^2Sc + \gamma Sc)\phi_1 + ScSr\theta_1'' = 0 \tag{22}$$

$$\phi_2'' - RSc\phi_2' - (2iM^2Sc + \gamma Sc)\phi_2 + ScSr\theta_2'' = 0 \tag{23}$$

where $H = \frac{B_0 h \sqrt{\sigma}}{\sqrt{\mu}}$ is the Hartmann number, $M = \frac{h\sqrt{\omega}}{\sqrt{\nu}}$ is frequency parameter and μ is dynamic viscosity.

The corresponding boundary conditions are:

$$\begin{aligned} u_0(0) &= Lu_0'(0), u_0(1) = -Lu_0'(1), u_1(0) = Lu_1'(0), u_1(1) \\ &= -Lu_1'(1), \theta_0(0) = -B_i[\theta_0(0) - 1], \\ \theta_0'(1) &= -B_i\theta_0(1), \theta_1(0) = -B_i\theta_1(0), \theta_1'(1) = -B_i\theta_1(1), \theta_2(0) \\ &= -B_i\theta_2(0), \\ \theta_2'(1) &= -B_i\theta_2(1), \phi_0'(0) = -N[\phi_0(0) - 1], \phi_0'(1) \\ &= -N\phi_0(1), \phi_1'(0) = -N\phi_1(0), \\ \phi_1'(1) &= -N\phi_1(1), \phi_2'(0) = -N\phi_2(0), \phi_2'(1) = -N\phi_2(1). \end{aligned} \tag{24}$$

By solving Eqs. (16)–(23) with the corresponding boundary conditions (24), one obtains

$$u_0 = A_2 e^{m_1 \eta} + A_1 e^{m_2 \eta} + \frac{1}{H^2} \tag{25}$$

$$u_1 = A_5 e^{m_3 \eta} + A_4 e^{m_4 \eta} + A_3 \tag{26}$$

$$\theta_0 = A_6 + A_7 e^{RPr\eta} + A_8 e^{2m_1 \eta} + A_9 e^{(m_1+m_2)\eta} + A_{10} e^{2m_2 \eta} \tag{27}$$

$$\begin{aligned} \theta_1 &= A_{11} e^{m_5 \eta} + A_{12} e^{m_6 \eta} + A_{13} e^{(m_1+m_3)\eta} + A_{14} e^{(m_1+m_4)\eta} \\ &+ A_{15} e^{(m_2+m_3)\eta} + A_{16} e^{(m_2+m_4)\eta} \end{aligned} \tag{28}$$

$$\begin{aligned} \theta_2 &= A_{17} e^{m_7 \eta} + A_{18} e^{m_8 \eta} + A_{19} e^{2m_3 \eta} + A_{20} e^{(m_3+m_4)\eta} \\ &+ A_{21} e^{2m_4 \eta} \end{aligned} \tag{29}$$

$$\begin{aligned} \phi_0 &= A_{22} e^{m_9 \eta} + A_{23} e^{m_{10} \eta} + A_{24} e^{RPr\eta} + A_{25} e^{2m_1 \eta} \\ &+ A_{26} e^{(m_1+m_2)\eta} + A_{27} e^{2m_2 \eta} + A_{28} \end{aligned} \tag{30}$$

$$\begin{aligned} \phi_1 &= A_{29} e^{m_{11} \eta} + A_{30} e^{m_{12} \eta} + A_{31} e^{m_5 \eta} + A_{32} e^{m_6 \eta} \\ &+ A_{33} e^{(m_1+m_3)\eta} + A_{34} e^{(m_1+m_4)\eta} + A_{35} e^{(m_2+m_3)\eta} \\ &+ A_{36} e^{(m_2+m_4)\eta} \end{aligned} \tag{31}$$

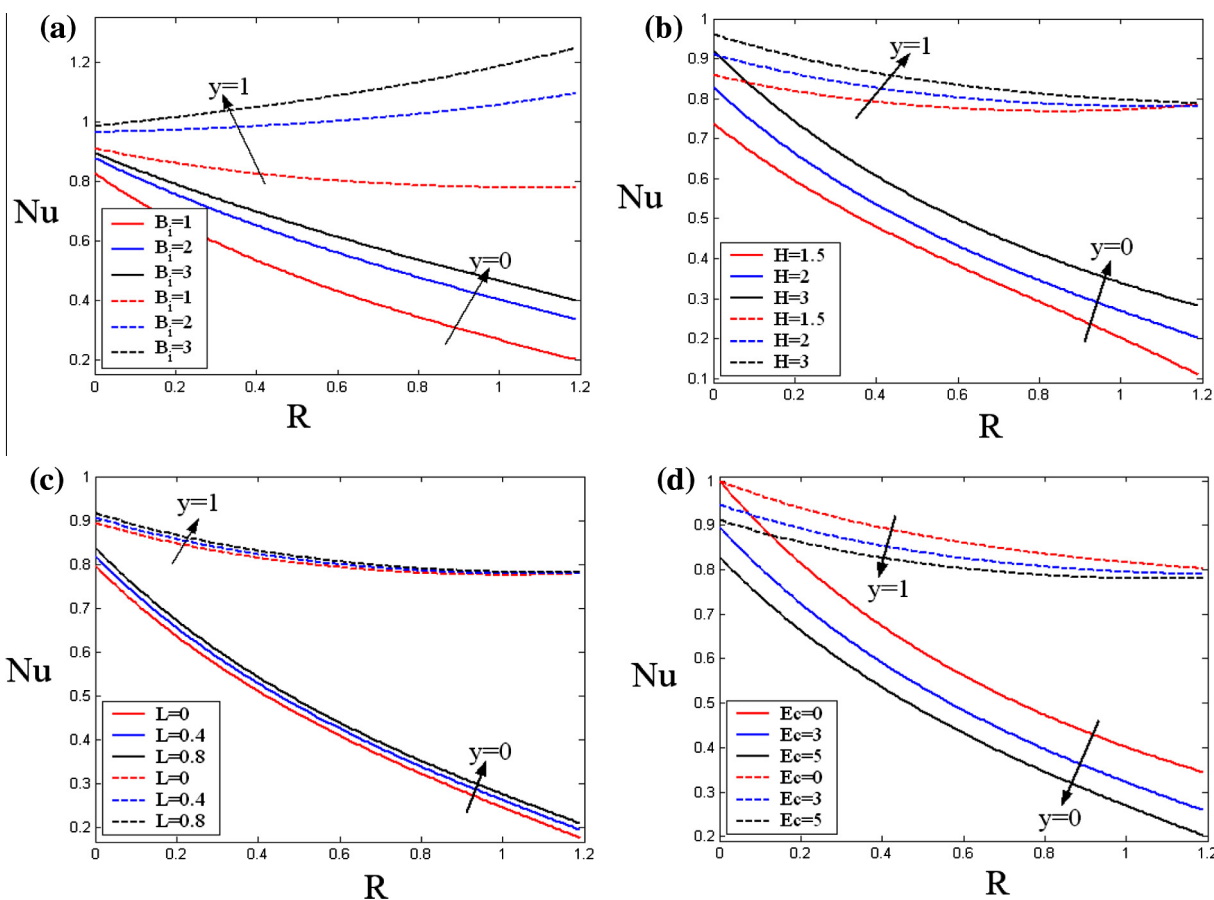


Figure 5 Nusselt number distribution for $\varepsilon = 0.01$, $\omega t = \pi/2$, $M = 5$, $Pr = 0.71$. (a) Effect of B_i when $Ec = 5$, $L = 0.06$, $H = 2$, (b) Effect of H when $B_i = 1$, $Ec = 5$, $L = 0.06$, (c) Effect of Ec when $H = 2$, $L = 0.06$, $B_i = 1$ and (d) Effect of L when $B_i = 1$, $Ec = 5$, $H = 2$.

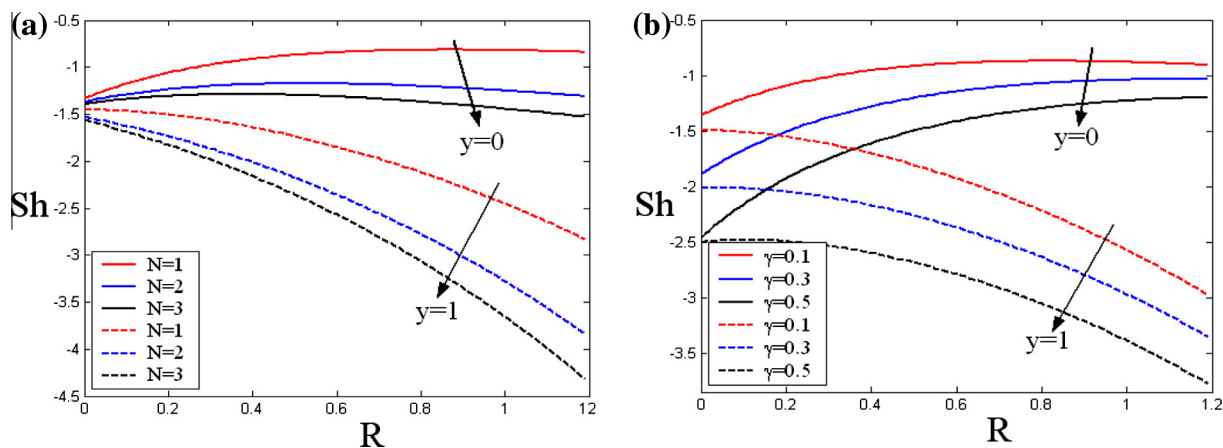


Figure 6 Sherwood number distribution for $Sr = 2$, $\omega t = \pi/2$, $M = 5$, $\varepsilon = 0.01$, $K_1 = 0.001$, $H = 2$, $Ec = 5$, $Pr = 0.71$, $R = 2$, $B_i = 1$, $L = 0.06$, $Sc = 0.62$. (a) Effect of N when, $\gamma = 0.3$ and (b) Effect of γ when $N = 1$, $Sr = 2$.

$$\phi_2 = A_{37}e^{m_{13}\eta} + A_{38}e^{m_{14}\eta} + A_{39}e^{m_{17}\eta} + A_{40}e^{m_{18}\eta} + A_{41}e^{2m_{13}\eta} + A_{42}e^{(m_{13}+m_{14})\eta} + A_{43}e^{2m_{14}\eta} \quad (32)$$

where m 's, A 's, B 's and D 's are constants given in Appendix A.

Further, the heat and mass transfer rates in terms of Nusselt number and Sherwood number at the walls respectively are defined as

$$Nu = -\left.\frac{\partial\theta}{\partial\eta}\right|_{\eta=0,1} \quad \text{and} \quad Sh = -\left.\frac{\partial\phi}{\partial\eta}\right|_{\eta=0,1} \quad (33)$$

4. Results and discussion

In order to get the physical insight of the problem, velocity, temperature, concentration, Nusselt number and Sherwood number distributions have been discussed by assigning numerical values to various parameters obtained in mathematical formulation of the problem and the results are shown graphically. Fig. 2a and b shows the influence of the Hartmann number H and slip parameter L on the velocity distribution. Fig. 2a shows that the velocity decreases with an increase of H . This is due to the fact that an increase in H increases the resistive force called Lorentz force which opposes the horizontal flow. Fig. 2b depicts the velocity distribution for different values of the slip parameter L . It can be observed that the velocity increases with an increase of L and the maximum is at the center of the channel. Fig. 3a–d elucidates the influence of the heat transfer Biot number B_i , the Hartmann number H , the Prandtl number Pr , and the cross flow Reynolds number R on the temperature distribution θ . Fig. 3a shows the effect of B_i on θ . It is noticed that θ decreases with an increase of B_i . Higher values of B_i inculcate higher degree of convective cooling at the channel walls thereby causing lower temperature at the channel walls and also in the bulk fluid. It is anticipated that as $B_i \rightarrow \infty$, the convective boundary conditions will become the prescribed wall temperature case Yao et al. (2011). Fig. 3b demonstrates that θ is an increasing function of H due to the fact that, the increase of H gives rise to the resistive force which has to increase the temperature of the fluid. Fig. 3c depicts that θ decreases for a given increase in Pr , which means viscous boundary layer is thicker than the thermal boundary layer. From Fig. 3d it is noticed that θ decreases with an increase of R .

Fig. 4a–d presents the effects of the mass transfer Biot number N , Soret number Sr , the chemical reaction parameter γ and the heat transfer Biot number B_i on the concentration distribution ϕ . Fig. 4a elucidates that ϕ increases with an increase of the mass transfer Biot number N . The similar behavior can be found when N is replaced by B_i (see Fig. 4d). Fig. 4b illustrates that ϕ is an increasing function of Sr . The influence of chemical reaction parameter γ on ϕ is shown in Fig. 4c. It is observed that ϕ decreases with an increase of γ .

Fig. 5a–d depicts the effects of B_i , H , Ec and L on the Nusselt number distribution Nu against R . Fig. 5a shows that for a given increase in B_i , Nu increases at both the walls. Similar conclusions can be drawn when B_i is replaced by H and L (see Figs. 4b and c). From Fig. 5d, it is observed that an increase of Ec decreases the heat transfer rate at both the walls. Fig. 6a and b demonstrates the effect of N and γ on Sherwood number distribution Sh against R . It is observed that Sh is a decreasing function of N and γ at both the walls.

5. Conclusions

This note deals with the analysis of the effects of Soret and chemical reaction on pulsating MHD viscous flow in a porous channel with convective boundary conditions. Analytical expressions are constructed for the velocity, temperature and concentration distributions. The main findings are summarized as follows:

- The temperature distribution decreases for a given increase in B_i , Pr and R , while it increases with an increase of H .
- The concentration distribution increases with an increase of the mass transfer Biot number N , Soret number Sr and the heat transfer Biot number B_i , while it decreases for a given increase in the chemical reaction parameter γ .
- The heat transfer rate increases with an increase of B_i and H , while it decreases with Ec and L at both the walls. The mass transfer rate decreases for a given increase in N and γ . It is expected that as $B_i \rightarrow \infty$ and $N \rightarrow \infty$, the convective boundary conditions will become the prescribed wall temperature and concentration case respectively.

- The results of hydrodynamic case can be recovered as a limiting case of our analysis by taking $H = 0$. Further, the results of Radhakrishnamacharya and Maiti (1977) in the absence mass diffusion can be captured as a special case of our analysis by taking $Bi \rightarrow \infty$, $N \rightarrow \infty$ and $L = 0$.

Acknowledgement

One of the authors (S.S.) gratefully acknowledges DST, Government of India for sanctioning a major research project under the grant number SR/SL.MS: 674/10.

Appendix A.

$$m_{1,2} = (R \pm \sqrt{R^2 + 4H^2})/2; \quad m_{3,4} \\ = (R \pm \sqrt{R^2 + 4(iM^2 + H^2)})/2$$

$$m_{5,6} = \frac{RPr \pm \sqrt{R^2 Pr^2 + 4iM^2 Pr}}{2}; \quad m_{7,8} \\ = \frac{RPr \pm \sqrt{R^2 Pr^2 + 8iM^2 Pr}}{2};$$

$$m_{9,10} = \frac{RSc \pm \sqrt{R^2 Sc^2 + 4\gamma Sc}}{2}; \quad l_1 = iM^2 Sc + \gamma Sc;$$

$$m_{11,12} = \frac{RSc \pm \sqrt{R^2 Sc^2 + 4l_1}}{2};$$

$$l_2 = 2iM^2 Sc + \gamma Sc; \quad m_{13,14} = \frac{RSc \pm \sqrt{R^2 Sc^2 + 4l_2}}{2};$$

$$A_1 = \frac{(Lm_1 + 1)e^{m_1} + (Lm_1 - 1)}{H^2[(L^2 m_1 m_2 + Lm_2 - Lm_1 - 1)e^{m_1} - (L^2 m_1 m_2 - Lm_2 + Lm_1 - 1)e^{m_2}]};$$

$$A_2 = \frac{-(Lm_2 - 1)A_1 + (1/H^2)}{(Lm_1 - 1)}; \quad A_3 = \frac{1}{iM^2 + H^2};$$

$$B_3 = \frac{-EcPrm_2^2 A_1^2}{4m_2^2 - 2RPrm_2};$$

$$A_4 = \frac{(Lm_3 + 1)e^{m_3} + (Lm_3 - 1)}{H^2[(L^2 m_3 m_4 + Lm_4 - Lm_3 - 1)e^{m_3} - (L^2 m_3 m_4 - Lm_4 + Lm_3 - 1)e^{m_4}]};$$

$$A_5 = \frac{A_3 - (Lm_4 - 1)A_4}{Lm_3 - 1}; \quad B_1 = \frac{-EcPrm_1^2 A_2^2}{4m_1^2 - 2RPrm_1};$$

$$B_2 = \frac{-2EcPrm_1 m_2 A_1 A_2}{(m_1 + m_2)^2 - RPr(m_1 + m_2)};$$

$$B_5 = [-B_i(B_1 + B_2 + B_3 - 1) - 2m_1 B_1 - (m_1 + m_2)B_2 \\ - 2m_2 B_3 - (B_i + RPr)B_4]/B_i;$$

$$B_6 = \frac{-2EcPrm_1 m_3 A_2 A_5}{(m_1 + m_3)^2 - RPr(m_1 + m_3) - iM^2 Pr};$$

$$B_7 = \frac{-2EcPrm_1 m_4 A_2 A_4}{(m_1 + m_4)^2 - RPr(m_1 + m_4) - iM^2 Pr};$$

$$B_8 = \frac{-2EcPrm_2 m_3 A_1 A_5}{(m_2 + m_3)^2 - RPr(m_2 + m_3) - iM^2 Pr};$$

$$B_9 = \frac{-2EcPrm_2 m_4 A_1 A_4}{(m_2 + m_4)^2 - RPr(m_2 + m_4) - iM^2 Pr};$$

$$n_1 = B_i\{B_6(e^{m_1+m_3} - e^{m_5}) + B_7(e^{m_1+m_4} - e^{m_5}) + B_8(e^{m_2+m_3} \\ - e^{m_5}) + B_9(e^{m_2+m_4} - e^{m_5})\};$$

$$n_2 = (m_1 + m_3)B_6(e^{m_1+m_3} - e^{m_5}) + (m_1 + m_4)B_7(e^{m_1+m_4} - e^{m_5}) \\ + (m_2 + m_3)B_8(e^{m_2+m_3} - e^{m_5}) \\ + (m_2 + m_4)B_9(e^{m_2+m_4} - e^{m_5}); \quad n_3 = (B_6 + B_i)(e^{m_5} - e^{m_6});$$

$$B_{10} = \frac{n_1 + n_2}{3};$$

$$B_{11} = \left[\frac{-B_i(B_6 + B_7 + B_8 + B_9) - (m_1 + m_3)B_6 - (m_1 + m_4)B_7}{B_7 - (m_2 + m_3)B_8 - (m_2 + m_4)B_9 - (m_6 + B_i)B_{10}} \right] / (m_6 + B_i);$$

$$B_{12} = \frac{-EcPrm_3^2 A_5^2}{4m_3^2 - 2RPrm_3 - 2iM^2 Pr};$$

$$B_{13} = \frac{-2EcPrm_3 m_4 A_4 A_5}{(m_3 + m_4)^2 - RPr(m_3 + m_4) - 2iM^2 Pr};$$

$$B_{14} = \frac{-EcPrm_4^2 A_4^2}{4m_4^2 - 2RPrm_4 - 2iM^2 Pr};$$

$$n_4 = B_i\{B_{12}(e^{2m_3} - e^{m_7}) + B_{13}(e^{m_3+m_4} - e^{m_7}) + B_{14}(e^{2m_4} - e^{m_7})\};$$

$$n_5 = 2m_3 B_{12}(e^{2m_3} - e^{m_7}) + (m_3 + m_4)B_{13}(e^{m_3+m_4} - e^{m_7}) \\ + 2m_4 B_{14}(e^{2m_4} - e^{m_7});$$

$$n_6 = (m_8 + B_i)(e^{m_7} - e^{m_8}); \quad B_{15} = \frac{n_4 + n_5}{6};$$

$$B_{16} = \left[\frac{-B_i(B_{12} + B_{13} + B_{14}) - 2m_3 B_{12} - (m_3 + m_4)B_{13}}{-2m_4 B_{14} - (m_8 + B_i)B_{15}} \right] / (m_5 + B_i);$$

$$D_1 = \frac{-ScSrR^2 Pr^2 B_4}{R^2 Pr^2 - R^2 ScPr - \gamma Sc}; \quad D_2 = \frac{-ScSrm_1^2 B_1}{4m_1^2 - 2RScm_1 - \gamma Sc};$$

$$B_4 = \left[\frac{B_i(B_1(e^{2m_1} - 1) + B_2(e^{m_1+m_2} - 1) + B_3(e^{2m_2} - 1)) + \\ 2m_1 B_1(e^{2m_1} - 1) + (m_1 + m_2)B_2(e^{m_1+m_2-1}) + 2m_2 B_3(e^{2m_2} - 1)}{(B_i + RPr)(1 - e^{RPr})} \right];$$

$$D_3 = \frac{-ScSr(m_1 + m_2)B_2}{(m_1 + m_2)^2 - RSc(m_1 + m_2) - \gamma Sc};$$

$$D_4 = \frac{-4ScSrm_2^2 B_3}{4m_2^2 - 2RScm_2 - \gamma Sc}; \quad D_5 = \frac{-K_1}{\gamma Sc};$$

$$n_7 = N[D_1(e^{RPr} - e^{m_9}) + D_2(e^{2m_1} - e^{m_9}) + D_3(e^{m_1+m_2} - e^{m_9}) + D_4(e^{2m_2} - e^{m_9}) + D_5(1 - e^{m_9}) - e^{m_9}];$$

$$n_8 = RPrD_1(e^{RPr} - e^{m_9}) + 2m_1D_2(e^{2m_1} - e^{m_9}) + (m_1 + m_2)D_3(e^{m_1+m_2} - e^{m_9}) + 2m_2D_4(e^{2m_2} - e^{m_9});$$

$$n_9 = (m_{10} + N)(e^{m_9} - e^{m_{10}}); \quad D_6 = \frac{n_7 + n_8}{n_9};$$

$$n_{10} = -N(D_1 + D_2 + D_3 + D_4 + D_5 - 1);$$

$$n_{11} = -RPr - 2m_1D_2 - (m_1 + m_2)D_3 - 2m_2D_4 - (m_{10} + N)D_6;$$

$$n_{12} = (m_9 + N);$$

$$D_7 = \frac{n_{10} + n_{11}}{n_{12}}; \quad D_8 = \frac{-ScSrm_5^2 B_{11}}{m_5^2 - RScm_5 - l_1};$$

$$D_9 = \frac{-ScSrm_6^2 B_{10}}{m_6^2 - RScm_6 - l_1};$$

$$D_{10} = \frac{-ScSr(m_1 + m_3)^2 B_6}{(m_1 + m_3)^2 - RSc(m_1 + m_3) - l_1};$$

$$D_{11} = \frac{-ScSr(m_1 + m_4)^2 B_7}{(m_1 + m_4)^2 - RSc(m_1 + m_4) - l_1};$$

$$D_{12} = \frac{-ScSr(m_2 + m_3)^2 B_8}{(m_2 + m_3)^2 - RSc(m_2 + m_3) - l_1};$$

$$D_{13} = \frac{-ScSr(m_2 + m_4)^2 B_9}{(m_2 + m_4)^2 - RSc(m_2 + m_4) - l_1};$$

$$n_{13} = N[D_8(e^{m_5} - e^{m_{11}}) + D_9(e^{m_6} - e^{m_{11}}) + D_{10}(e^{m_1+m_3} - e^{m_{11}}) + D_{11}(e^{m_1+m_4} - e^{m_{11}}) + D_{12}(e^{m_2+m_3} - e^{m_{11}}) + D_{13}(e^{m_2+m_4} - e^{m_{11}})];$$

$$n_{14} = m_5D_8(e^{m_5} - e^{m_{11}}) + m_6D_9(e^{m_6} - e^{m_{11}}) + (m_1 + m_3)D_{10}(e^{m_1+m_3} - e^{m_{11}}) + (m_1 + m_4)D_{11}(e^{m_1+m_4} - e^{m_{11}}) + (m_2 + m_3)D_{12}(e^{m_2+m_3} - e^{m_{11}}) + (m_2 + m_4)D_{13}(e^{m_2+m_4} - e^{m_{11}});$$

$$n_{15} = (m_{12} + N)(e^{m_{11}} - e^{m_{12}}); \quad D_{14} = \frac{n_{13} + n_{14}}{n_{15}};$$

$$n_{16} = -N(D_8 + D_9 + D_{10} + D_{11} + D_{12} + D_{13});$$

$$n_{17} = -m_5D_8 - m_6D_9 - (m_1 + m_3)D_{10} - (m_1 + m_4)D_{11} - (m_2 + m_3)D_{12} - (m_2 + m_4)D_{13} - (m_{12} + N)D_{14};$$

$$n_{18} = m_{11} + N;$$

$$D_{15} = \frac{n_{16} + n_{17}}{n_{18}}; \quad D_{16} = \frac{-ScSrm_7^2 B_{16}}{m_7^2 - RScm_7 - l_2};$$

$$D_{17} = \frac{-ScSrm_8^2 B_{15}}{m_8^2 - RScm_8 - l_2};$$

$$D_{18} = \frac{-4ScSrm_3^2 B_{12}}{4m_3^2 - 2RScm_3 - l_2}; \quad D_{19} = \frac{-4ScSrm_3^2 B_{12}}{4m_3^2 - 2RScm_3 - l_2};$$

$$D_{20} = \frac{-4ScSrm_4^2 B_{12}}{4m_4^2 - 2RScm_4 - l_2};$$

$$n_{19} = N[D_{16}(e^{m_7} - e^{m_{13}}) + D_{17}(e^{m_8} - e^{m_{13}}) + D_{18}(e^{2m_3} - e^{m_{13}}) + D_{19}(e^{m_3+m_4} - e^{m_{13}}) + D_{20}(e^{2m_4} - e^{m_{13}})];$$

$$n_{20} = m_7D_{16}(e^{m_7} - e^{m_{13}}) + m_8D_{17}(e^{m_8} - e^{m_{13}}) + 2m_3D_{18}(e^{2m_3} - e^{m_{13}}) + (m_3 + m_4)D_{19}(e^{m_3+m_4} - e^{m_{13}}) + 2m_4D_{20}(e^{2m_4} - e^{m_{13}}); \quad D_{22} = \frac{n_{22} + n_{23}}{n_{14}}$$

$$n_{21} = (m_{14} + N)(e^{m_{13}} - e^{m_{14}}); \quad D_{21} = \frac{n_{19} + n_{20}}{n_{21}};$$

$$n_{22} = -N(D_{16} + D_{17} + D_{18} + D_{19} + D_{20});$$

$$n_{23} = -m_7D_{16} - m_8D_{17} - 2m_3D_{18} - (m_3 + m_4)D_{19} - 2m_4D_{20} - (m_{14} + N)D_{21}; \quad n_{24} = m_{13} + N;$$

References

- Akbar, N.S., 2013. MHD Eyring Prandtl fluid flow with convective boundary conditions in small intestines. *Int. J. Biomath.* 6, 1350034.
- Akbar, N.S., Nadeem, S., 2012. Characteristics of heating scheme and mass transfer on the peristaltic flow for an Eyring-Powell fluid in an endoscope. *Int. J. Heat Mass Transfer* 55, 375–383.
- Akbar, N.S., Haya, T., Nadeem, S., Obaidat, S., 2012a. Peristaltic flow of Tangent hyperbolic fluid in an inclined asymmetric channel with slip and heat transfer. *Prog. Comput. Fluid Dyn.* 12, 363–374.
- Akbar, N.S., Nadeem, S., Haya, T., 2012b. Simulation of thermal and velocity slip on the peristaltic flow of a Johnson–Segalman fluid in an inclined asymmetric channel. *Int. J. Heat Mass Transfer* 55, 5495–5502.
- Beavers, G.S., Joseph, D.D., 1967. Boundary conditions at a naturally permeable wall. *J. Fluid Mech.* 30, 197–207.
- Berman, A.S., 1953. Laminar flow in channel with porous walls. *J. Appl. Phys.* 24, 1232–1235.
- Chamka, A.J., Nakhi, A.B., 2008. MHD mixed convection-radiation interaction along a permeable surface immersed in a porous medium in the presence of Soret and Dufour's effects. *Heat Mass Transfer* 44, 845–856.
- Chellam, S., Wiesner, M.R., Dawson, C., 1992. Slip at a uniformly porous boundary: effect on fluid flow and mass transfer. *J. Eng. Math.* 26, 481–492.
- Chen, Y.L., Zhu, K.E., 2008. Couette–Poiseuille flow of Bingham fluids between to porous parallel plates with slip conditions. *J. Non-Newtonian Fluid Mech.* 153, 1–11.
- Chinyoka, T., Makinde, O.D., 2011. Analysis of transient generalized Couette flow of a reactive variable viscosity third-grade liquid with asymmetric convective cooling. *Math. Comput. Modelling* 54, 160–174.
- Cox, S.M., 1991. Two dimensional flow of a viscous fluid in a channel with porous walls. *J. Fluid Mech.* 227, 1–33.
- Dursunkaya, Z., Worek, W.M., 1992. Diffusion-thermo and thermal-diffusion effects in transient and steady natural convection from vertical surface. *Int. J. Heat Mass Transfer* 35, 2060–2065.
- Hayat, T., Hina, S., Ali, N., 2010. Simultaneous effects of slip and heat transfer on the peristaltic flow. *Commun. Nonlinear Sci. Numer. Simulat.* 15, 1526–1537.

- Hayat, T., Hina, S., Hendi, A.A., 2012. Slip effects on peristaltic transport of a Maxwell fluid with heat and mass transfer. *J. Mech. Med. Biol.* 12, 1250001.
- Hayat, T., Nawaz, M., Asghar, S., Mesloub, S., 2011. Thermal-diffusion and diffusion-thermo effects on axisymmetric flow of a second grade fluid. *Int. J. Heat Mass Transfer* 54, 3031–3041.
- Makinde, O.D., 2009. Thermal stability of a reactive viscous flow through a porous-saturated channel with convective boundary conditions. *Appl. Therm. Eng.* 29, 1773–1777.
- Malathy, T., Srinivas, S., 2008. Pulsating flow of hydromagnetic fluid between permeable beds. *Int. Commun. Heat Mass Transfer* 35, 681–688.
- Mustafa, M., Abbasbandy, S., Hina, S., Hayat, T., 2014. Numerical investigation on mixed convective peristaltic flow of fourth grade fluid with Dufour and Soret effects. *J. Taiwan Inst. Chem. Eng.* 45, 308–316.
- Nadeem, S., Mehmood, R., Akbar, N.S., 2014. Optimized analytical solution for oblique flow of Casson-nanofluid with convective boundary conditions. *Int. J. Therm. Sci.* 78, 90–100.
- Narayana, P.A.L., Murthy, P.V.S.N., Gorla, R.S.R., 2008. Soret-driven thermosolutal convection induced by inclined thermal and solutal gradients in a shallow horizontal layer of a porous medium. *J. Fluid Mech.* 612, 1–19.
- Radhakrishnamacharya, G., Maiti, M.K., 1977. Heat transfer to pulsatile flow in a porous channel. *Int. J. Heat Mass Transfer* 20, 171–173.
- Srinivas, S., Reddy, A.S., Ramamohan, T.R., 2012. A study on thermal-diffusion and diffusion-thermo effects in a two-dimensional viscous flow between slowly expanding or contracting walls with weak permeability. *Int. J. Heat Mass Transfer* 55, 3008–3020.
- Terrill, R.M., 1964. Laminar flow in a uniformly porous channel. *Aeronaut Q.* 15, 299–310.
- Xinhui, S., Liacun, Z., Xuehui, C., Xinxin, Z., Limer, C., Min, L., 2012. The effects of slip velocity on a micropolar fluid through a porous channel with expanding or contracting walls. *Comput. Methods Biomech. Biomed. Eng.*, 1–10.
- Yao, S., Fang, T., Zhong, Y., 2011. Heat transfer of a generalized stretching/shrinking wall problem with convective boundary conditions. *Commun. Nonlinear Sci. Numer. Simulat.* 16, 752–760.